

Analysis of polarization transformations by a planar chiral array of complex-shaped particles

Sergey L Prosvirnin¹ and Nikolay I Zheludev²

¹ Institute of Radio Astronomy, Kharkov 61002, Ukraine

² Optoelectronics Research Centre, University of Southampton, Southampton SO17 1BJ, UK

E-mail: prosvirn@rian.kharkov.ua and niz@orc.soton.ac.uk

Received 25 September 2008, accepted for publication 27 November 2008

Published 6 May 2009

Online at stacks.iop.org/JOptA/11/074002

Abstract

Vectorial relations of field amplitudes are derived from the Lorentz lemma applied to electromagnetic fields at direct and reversed scenarios of a wave diffraction on a doubly-periodic planar array. Biorthogonality of polarization eigenstates of the waves propagating in opposite directions is shown with reference to a wave channel formed by an incident wave and a diffraction order. For a planar chiral array, an essential difference in polarization transformations of propagated waves is ascertained in the direct wave channel and in the reversed one. Numerical data are presented to demonstrate the polarization transformations by both transmitting and reflecting planar chiral arrays. A difference in polarization eigenstates inherent to a planar chiral array and a bulk chiral medium is noticed.

Keywords: array, diffraction, polarization, chirality

1. Introduction

Singly-periodic planar arrays consisting of straight wires or metal strips have a long history of applications as quasi-optical polarizing devices. Their properties are well known.

Doubly-periodic planar arrays composed of highly symmetric non-chiral elements were considered mainly as frequency selective surfaces [1, 2]. Electromagnetic properties of chiral scatterers [3] and structures consisting of complex-shaped particles (such as C-, S- and Ω -shaped particles) were analyzed as potentially useful structures for metamaterials and photonics applications [4–7]. A generalized scattering matrix theory was developed in [8, 9] for analysis of scattering by a doubly-periodic array of arbitrary-shaped planar elements. However, polarization transformations by such structures have not yet been comprehensively studied.

So-called planar chiral structures are of particular interest among the doubly-periodic arrays. Planar chiral structures consist of flat elements and they have no axis of symmetry in their plane [10].

Polarization transformations occurring during scattering by planar chiral arrays are of great interest [11, 12]. In particular, they are attractive for applications in quasi-optical

isolators. For a direct ray way the polarization transformation at a wave scattering by a planar chiral array into a diffraction order is different from that for the reversed way. Planar chiral arrays differ markedly from non-chiral arrays due to this property. Both structural chirality of an array arrangement and chirality of individual elements of the array give rise to the polarization effects.

The important properties of polarization transformations may be derived from the reciprocity principle for a three-dimensional electromagnetic wave scattering by a doubly-periodic complex planar structure. They are quite unusual in comparison with the properties of singly-periodic arrays. We will analyze the polarization changes of light diffracted on a planar chiral periodic array from the standpoint of the reciprocity principle and find biorthogonality in the polarization eigenstates for the waves diffracting through the array and reflected by the array in opposite directions.

In electromagnetic theory a common definition of the reciprocity principle is formulated in the form of the Lorentz lemma [13]. If the Lorentz lemma is held in some volume, the scattering structure lying in the volume is reciprocal. It is a quite general form of electromagnetic phenomenon classification. All linear electromagnetic systems constituted

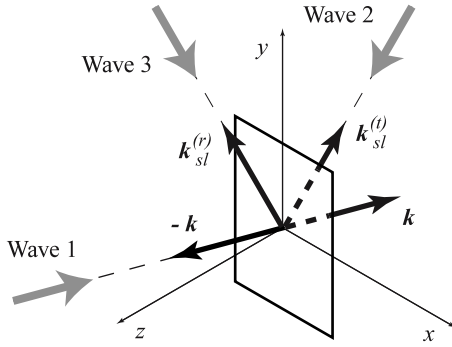


Figure 1. A coordinate system and waves in the direct and reversed scenarios for the transmitted and reflected fields.

by materials characterized by symmetric tensors of permittivity and permeability fall into this definition of reciprocity (the system can be lossy or lossless, homogeneous or non-homogeneous).

However, from the practical standpoint it is also important to classify electromagnetic effects with respect to the results of two experiments in which the directions of electromagnetic wave propagation are mutually opposite [14]. If such experiments yield different results, the effect may be called asymmetric, but nevertheless compatible with the reciprocity principle. The difference in polarization transformations for a partial wave diffracted on a doubly-periodic planar chiral array in the opposite directions is a recently discovered example of such an asymmetric effect [15].

The main aim of the paper is to present the results of a detailed study of polarization transformations caused by planar chiral array scattering in a resonance frequency range.

2. Reciprocity theorems for wave diffraction by a planar array

From the region $z > 0$ the plane electromagnetic wave

$$\mathbf{E}^{(1i)} = e^{(1)} \exp(-i\mathbf{k}\mathbf{r}) \quad (1)$$

is incident on a periodic structure placed in free space within the layer $-h < z < 0$ parallel to the xy plane (see figure 1: wave 1). Here $e^{(1)}$ is a unit polarization vector, $\mathbf{k} = \mathbf{k}_\perp - e_z(k^2 - k_\perp^2)^{1/2}$ is a wavevector, $\mathbf{k}_\perp = e_x k \sin \theta_i \cos \phi_i + e_y k \sin \theta_i \sin \phi_i$ is a component of \mathbf{k} transverse to the axis z , ϕ_i and θ_i are the azimuth and the polar angle of the incidence direction (the angle of incidence is $\pi - \theta_i$), $k = 2\pi/\lambda$, and vectors e_x , e_y and e_z are unit basis vectors along the axes x , y and z . We assume an $\exp(i\omega t)$ time dependence. For simplicity of notation the time multiplier has been dropped in (1) and below. The incident wave is assumed to be a non-evanescent plane wave.

In brief, below we will only consider periodic structures with a rectangular cell. The field outside of the periodic structure is a superposition of partial diffracted waves

propagating away from the array and along the array's plane:

$$\mathbf{E}^{(1)} = \begin{cases} \mathbf{E}^{(1i)} + \sum_{q,p=-\infty}^{\infty} \mathbf{a}_{qp}^{(1)} \exp(-i\mathbf{k}_{qp}^{(r)}\mathbf{r}), & z > 0, \\ \sum_{q,p=-\infty}^{\infty} \mathbf{b}_{qp}^{(1)} \exp(-i\mathbf{k}_{qp}^{(l)}(\mathbf{r} + e_z h)), & z < -h, \end{cases} \quad (2)$$

where $\mathbf{a}_{qp}^{(1)}$ and $\mathbf{k}_{qp}^{(r)} = \mathbf{k}_\perp + \mathbf{g}_{qp} + e_z \gamma_{qp}$ ($\mathbf{b}_{qp}^{(1)}$ and $\mathbf{k}_{qp}^{(l)} = \mathbf{k}_\perp + \mathbf{g}_{qp} - e_z \gamma_{qp}$) are amplitudes and wave vectors of diffracted partial waves of the reflected (transmitted) field, $\mathbf{g}_{qp} = 2\pi(e_x q/d_x + e_y p/d_y)$, d_x and d_y are the structure period sizes, and $\gamma_{qp} = (k^2 - |\mathbf{k}_\perp + \mathbf{g}_{qp}|^2)^{1/2}$, $\text{Im} \gamma_{qp} \leq 0$. The diffraction of wave 1 will be referred to as the *direct* diffraction scenario.

Let us now define the *reversed* diffraction scenario. In the reversed scenario we will consider a wave propagating towards the array in the direction opposite to one of the non-evanescent waves, diffracted in the direct scenario. For instance, this may be a partial wave of the direct diffraction scenario with indexes $q = s$ and $p = l$:

$$\mathbf{E}^{(2i)} = e^{(2)} \exp(i\mathbf{k}_{sl}^{(l)}(\mathbf{r} + e_z h)). \quad (3)$$

The wave approaches the structure from the region $z < -h$ along the direction $-\mathbf{k}_{sl}^{(l)}$ (see figure 1: wave 2). The incident wave $\mathbf{E}^{(2i)}$ creates its own diffraction pattern $\mathbf{E}^{(2)}$. One of the partial diffracted waves of this field will then propagate in the direction exactly opposite to the incident wave $\mathbf{E}^{(1i)}$ direction. This diffracted wave has indices sl and amplitude $\mathbf{b}_{sl}^{(2)}$. Therefore, the waves of the direct and reversed diffraction scenarios propagate in the opposite directions along the same wave channel consisting of an incident wave and a single partial diffracted wave.

We will suppose that the periodic structure has no nonlinear and non-reciprocal elements. The Lorentz reciprocity lemma [13] applied to the field superposition in the volume bounded by planes $x = \pm d_x/2$, $y = \pm d_y/2$, $z = z_1 > 0$ and $z = z_2 < -h$ may be written in the following form:

$$\oint_S \{[\mathbf{E}^{(1)} \times \mathbf{H}^{(2)}]_N - [\mathbf{E}^{(2)} \times \mathbf{H}^{(1)}]_N\} ds = 0 \quad (4)$$

where S is a surface enclosing the volume and N denotes the component of the vector product, that is perpendicular to surface S . By direct inspection it may be shown that the following relation results from the Lorentz lemma in *transmissive* configuration:

$$\gamma_{00}(e^{(1)} \cdot \mathbf{b}_{sl}^{(2)}) = \gamma_{sl}(e^{(2)} \cdot \mathbf{b}_{sl}^{(1)}). \quad (5)$$

Similarly, for wave 3 (see figure 1):

$$\mathbf{E}^{(3i)} = e^{(3)} \exp(i\mathbf{k}_{sl}^{(r)}\mathbf{r}) \quad (6)$$

we can derive the following relation between amplitudes $\mathbf{a}_{sl}^{(1)}$ and $\mathbf{a}_{sl}^{(3)}$ of the partial waves diffracted in the *reflective* configuration:

$$\gamma_{00}(e^{(1)} \cdot \mathbf{a}_{sl}^{(3)}) = \gamma_{sl}(e^{(3)} \cdot \mathbf{a}_{sl}^{(1)}) \quad (7)$$

where $\alpha_{sl}^{(3)}$ is the amplitude of the partial wave propagating along $-\mathbf{k}$ in a reflected field resulting from the diffraction of wave 3. The diffraction of wave (6) will be referred to as the reversed diffraction scenario in a reflected field.

Formulae (5) and (7) represent the fundamental relations, imposed by the reciprocity theorem, for the fields diffracted along the opposite directions of the same wave channel and should be valid for both lossy and lossless volumetric and infinitely thin arrays with any interior geometry of the periodic cell. They are particularizations of the general principle of reciprocity addressed by de Hoop [14] for the case of electromagnetic wave diffraction by planar doubly-periodic arrays. To the best of our knowledge, we cannot refer to any previous publications of these relations in connection with a vectorial wave diffraction by doubly-periodic arrays.

3. Matrices for diffraction in transmission and reflection

The incident wave and waves diffracted in transmission and reflection will be considered in a spherical coordinate system with a polar axis directed along z . In the spherical coordinate system the polarization vector $e^{(1)}$ of incident wave $E^{(1i)}$ is

$$e^{(1)} = e_\theta e_{\theta_1}^{(1)} + e_\phi e_{\phi_1}^{(1)} \quad (8)$$

where e_θ and e_ϕ are the unit basis vectors and polar direction e_ρ is along \mathbf{k} . The corresponding coordinates are designated by indexes θ_1 and ϕ_1 . The amplitude $b_{sl}^{(1)}$ of the transmitted field will be considered in the basis $e_\theta^{(1)}$, $e_\phi^{(1)}$ and $e_\rho^{(1)}$ constructed at the vector $\mathbf{k}_{sl}^{(1)}$. The corresponding coordinates θ and ϕ will be designated by indexes θ_2 and ϕ_2 .

The polarization vector $e^{(2)}$ of incident wave $E^{(2i)}$ and transmitted field amplitude $b_{sl}^{(2)}$ will be presented in the bases whose radial unit vectors are directed along $-\mathbf{k}_{sl}^{(1)}$ and $-\mathbf{k}$. For the reversed diffraction scenario the basis set of vectors is $e_\theta^{(1)}$, $-e_\phi^{(1)}$ and e_θ , $-e_\phi$ for the incident and diffracted waves correspondingly.

Let us now introduce a matrix operator T_+ relating the vectorial amplitude of the incident wave $E^{(1i)}$ to the sl -diffracted wave in the direct scenario:

$$b_{sl}^{(1)} = T_+ e^{(1)} \quad (9)$$

where

$$T_+ = \begin{pmatrix} t_{\theta_2\theta_1} & t_{\theta_2\phi_1} \\ t_{\phi_2\theta_1} & t_{\phi_2\phi_1} \end{pmatrix}. \quad (10)$$

Similarly, operator T_- corresponds to the reversed scenario:

$$b_{sl}^{(2)} = T_- e^{(2)}. \quad (11)$$

Below, the indexes sl will be dropped to simplify the notation. As the elements of matrices T_+ and T_- are coupled by equality (5), it may be shown that

$$T_- = \xi \begin{pmatrix} t_{\theta_2\theta_1} & -t_{\phi_2\theta_1} \\ -t_{\theta_2\phi_1} & t_{\phi_2\phi_1} \end{pmatrix} \quad (12)$$

where $\xi = \gamma_{sl}/\gamma_{00}$.

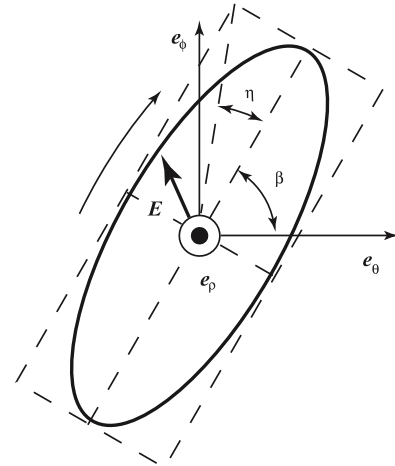


Figure 2. A definition of the polarization parameters: β is the azimuth of polarization; η is the ellipticity angle, the positive and negative sign of η corresponds to right-handed polarization (i.e. E rotates clockwise as is shown by the arrow in the figure) and left-handed polarization for observation opposite to a wave propagation direction.

All the above expressions of the electric field components are defined in the right-hand frames of the spherical coordinate systems. However, for the sake of comparison, it is convenient to present polarization parameters of the incident and diffracted waves of the reversed scenario in the same coordinate systems of the direct scenario. For vectorial amplitudes of the reversed scenario expressed in the bases of the direct scenario, the transmission matrix has the form $\xi T_+'$, where the prime denotes the transposition of the matrix. Thus an expression

$$b^{(2)} = \xi T_+' e^{(2)} \quad (13)$$

is valid for the reversed scenario vectors presented in the bases of the direct scenario.

As we are concerned with the polarization state of an electromagnetic wave, we will define polarization azimuth β and the ellipticity angle η (see figure 2) from the field amplitude using the standard definitions [16]: $\tan 2\beta = s_2/s_1$, $\sin 2\eta = s_3/s_0$, where s_i are the Stokes parameters calculated from the components of the electric field in the right-hand orthogonal frame. In the definition of the Stokes parameters it is assumed that ρ axis of the frame coincides with the wave propagation direction.

The bases of the direct diffraction scenario are suitable to calculate a polarization azimuth and an ellipticity angle of the scenario's waves. However, they are not appropriate immediately for azimuth and ellipticity calculation of the reversed scenario waves. The last follows from the above-mentioned frame definition for the Stokes parameter calculation.

Now we shall convert the formulae for polarization characteristics of the waves in the reversed scenario to the coordinate frames of the direct scenario. Let $E = \mathbf{u} \exp(-i\mathbf{k}_{sl}^{(1)}(\mathbf{r} + \mathbf{e}_z h))$ be a plane wave propagating away from the periodic structure along the direction $\mathbf{k}_{sl}^{(1)}$. Its polarization characteristics may be determined from the components of

vector $\mathbf{u} = e_{\theta}^{(i)} u_{\theta_2} + e_{\phi}^{(i)} u_{\phi_2}$ in the basis $e_{\theta}^{(i)}, e_{\phi}^{(i)}$. Now a wave $\tilde{\mathbf{E}} = \mathbf{u}^* \exp(ik_{sl}^{(i)}(\mathbf{r} + e_z h))$ propagates opposite to the direction of $\mathbf{k}_{sl}^{(i)}$ (here the asterisk denotes complex conjugation). It is essential that the Stokes parameters and consequently polarization azimuth and ellipticity of this wave are the same as the ones of wave \mathbf{E} . As a result of wave $\tilde{\mathbf{E}}$ diffraction by the periodic structure, the diffracted wave propagates along $-\mathbf{k}$ in the region corresponding to $z > 0$. Its vectorial amplitude is $\xi T'_+ \mathbf{u}^*$ as follows from (13). The polarization characteristics of this wave may be found from components of vector $\mathbf{v} = e_{\theta} v_{\theta_1} + e_{\phi} v_{\phi_1} = (\xi T'_+ \mathbf{u}^*)^*$ in the basis e_{θ}, e_{ϕ} .

Therefore, the reversed diffraction scenario may be analyzed using an expression

$$\mathbf{v} = \xi T_+^{\dagger} \mathbf{u} \quad (14)$$

where $T_+^{\dagger} = (T'_+)^*$ is an adjoint matrix operator of T_+ . We supposed here that the vectors \mathbf{u} and \mathbf{v} are written in the coordinates of the direct scenario and they are complex conjugated amplitudes of incident and diffracted fields correspondingly. The polarization characteristics of the reversed scenario incident wave and diffracted one may be calculated from components of vectors \mathbf{u} and \mathbf{v} .

Similarly, the matrix operator ξR_+^{\dagger} defines the polarization transformation in the reversed diffraction scenario in reflective configuration.

3.1. Polarization eigenstates

Eigenvectors of transmission and reflection matrices define the polarization states of the incident and diffracted waves, which do not change through diffraction. Below, these states will be called diffraction polarization eigenstates. As the matrix operators of wave transformation are mutually adjoint for the direct and reversed scenarios, their eigenvectors are *biorthogonal* [17]. Thus, polarization eigenstates corresponding to matrix T_+^{\dagger} are orthogonal to eigenstates corresponding to matrix ξT_+ . Similarly, eigenvectors of R_+ are orthogonal to those of ξR_+^{\dagger} and polarization eigenstates of the direct and reversed scenarios of reflective configuration are biorthogonal too.

The orthogonality of two polarization states means that in the coordinate frame of the direct scenario the corresponding polarization azimuths are perpendicular while ellipticity angles are equal in absolute values but opposite in signs. Therefore, the polarization eigenstates in the direct and reversed scenarios presented in the coordinate frame of the direct scenario can be different. Such a situation takes place if the complex matrix T_+ or the matrix R_+ of reflective configuration is an asymmetric matrix.

If we compare the orthogonal polarization eigenstates of waves propagating in opposite directions in the direct and reversed diffraction scenarios by projecting their polarization ellipses on a plane perpendicular to the ray, we will see that their main axes are orthogonal. We will also see that the electric field vectors tracing the identical ellipses rotate in the same direction, when observed from any side of the plane.

4. Analysis of polarization transformations

A set of consequences follows from the biorthogonality of eigenvectors. Firstly, polarization eigenstates of the direct and reversed scenarios correspond to two pairs of antipode points on a Poincaré sphere [16]. For any polarization eigenstate of the direct scenario depicted by a point on a Poincaré sphere, one can find the orthogonal polarization eigenstate of the reversed scenario in the antipode point. In general, the point representing the eigenstate in the direct scenario is an antipode to one of the points, which represents the eigenstates of the reversed scenario. The pairs of points corresponding to the direct and reversed diffraction scenarios may coincide.

Further, if the periodic structure is planar chiral that resulted from either structural chirality of the array arrangement or the array composition of chiral-shaped particles, the polarization eigenstates of direct and reversed transmission scenarios are different except for the scenarios based on a main (i.e. zero) diffraction order in certain configurations discussed below. Therefore, the diffraction leads to essentially different polarization transformations in the direct and reversed scenarios for this kind of array.

4.1. Array symmetry and general properties of polarization transformations

In general, the transmission and reflection matrices for periodic structures of complex-shaped particles have no symmetry. However, the reflection matrix of a normally incident wave into the main diffraction order is a symmetric matrix in the xy coordinate frame related to the array plane. Actually, the corresponding direct and reversed scenarios of reflection are indistinguishable and therefore the reflection matrix and its transposed one are coincident. In general, the transmission matrix has no symmetry as before.

Besides the normal incidence and normal diffraction, let us suppose now that a planar array consists of infinitely thin perfectly conducting elements placed in the plane $z = 0$ on a dielectric plane-parallel substrate with a thickness h . The substrate may be lossless or lossy dielectric. Because a tangential electric field is continuous in planes $z = 0$ and $-h$, the symmetry of the transmission matrix follows from the symmetry of the reflection one.

Furthermore, let us assume that this array has a fourfold symmetry relative to its normal. In particular, it may be a planar chiral array. It is evident that the transmission matrix of the normally incident wave to the main diffraction order has identical diagonal elements. The antisymmetry of the transmission matrix is also a consequence of the fourfold symmetry of the array. Thus the transmission matrix is symmetric on the one hand and it is antisymmetric on the other hand. Therefore, non-diagonal matrix elements are equal to zero and the polarization of the field of the main diffraction order is the same as polarization of an incident wave. Thus, the fourfold symmetry array of planar particles does not rotate the polarization of the normal incident wave in the main diffraction order. Numerical data obtained for arrays of infinitely thin rosettes placed on a substrate confirm this conclusion.

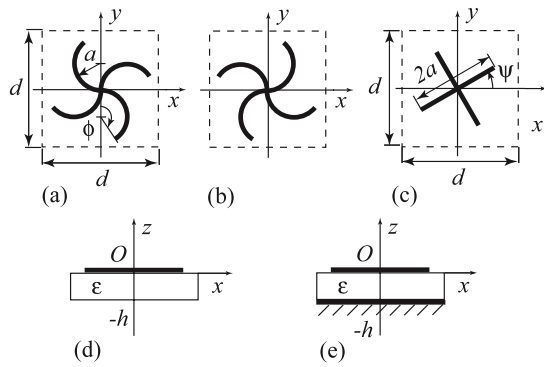


Figure 3. Structural elements of the arrays: right-handed rosette (a), left-handed rosette (b), straight cross (c) and the kinds of substrates: dielectric slab (d) and dielectric slab placed on a metal background (e).

It may be noticed that the polarization eigenstates are linear polarizations in the diffraction of a normally incident wave to the main diffraction order by a free standing array of infinitely thin perfectly conducting arbitrary-shaped patches placed in the array plane. This result is a rigorous consequence of a sign definiteness of a real part of the reflection matrix and its symmetry (see [18]).

Finally, the biorthogonality of polarization eigenstates is a property of wave diffraction by any planar arrays including arrays with a finite thickness and conductivity of metal elements. However, analysis of polarization transformations by such arrays is beyond the scope of this work. Let us mention here only that the transmission of a normally incident wave in the main diffraction order by a fourfold symmetry array of finite thickness conductive elements placed on a substrate is accompanied with a polarization rotation [19, 20]. The rotation is the same in both direct and reversed scenarios of transmission as the rotation by a layer of 3D chiral particles. But the same free-standing pattern (without substrate) is a symmetrical planar chiral structure and polarization rotation is not observed [19] as follows from the reciprocity principle.

4.2. Numerical analysis of polarization transformations by planar chiral arrays

Numerical analysis of the electromagnetic wave diffraction by the arrays of rosette-shaped metal strip particles and straight crosses (see figure 3) has been carried out. The array of rosettes is a planar chiral structure due to chirality of the particles. The array of crosses can be a planar chiral or non-chiral structure, depending on a symmetric or asymmetric arrangement of the crosses. Partly transparent and fully reflected kinds of arrays have been analyzed. They are the arrays placed on a dielectric substrate and a thin metal-background dielectric slab correspondingly. Polarization characteristics and an intensity of the field have been studied in the direct and reversed diffraction scenarios for different wave channels formed by the incident wave and some diffraction order.

The results presented below relate to the rosettes and the straight crosses arranged in the square cell arrays with the

period $d_x = d_y = 4$ mm. The width of the infinitely thin perfectly conducting strips of the rosettes was assumed to be 0.05 mm, radius $a = 1$ mm and bending angle $\phi = 120^\circ$. The array substrate with relative permittivity $\epsilon = 3$ and relative permeability $\mu = 1$ has thickness $h = 0.25$ mm. Enantiomorphic, left and right forms of the structure were obtained by using left and right forms of the rosette. The strip width of crosses was the same and the strip length of crosses was assumed to be $2a = 3$ mm.

The fields, intensities and polarization characteristics including polarization eigenstates of the electromagnetic wave diffracted by the plano-chiral arrays were calculated by the well-established method described in [21]. The method is based on a method of moments solution of a vectorial integral equation for the surface current induced by the electromagnetic field on the array elements. The equation is derived with boundary conditions that assume a zero value for the tangential component of the electric field on the metal strips. The numerical method does not explicitly use the Lorentz lemma; thus the validity of (14) for the reversed scenario was confirmed numerically as one of the tests to verify the code.

The Stokes parameters were calculated for analysis of an intensity and the polarization characteristics of diffracted waves. The intensity of a field was found as s_0 , and the polarization azimuth β and degree of ellipticity η were calculated using the above-mentioned standard definitions.

4.2.1. Main diffraction order. The transmission matrix T_+ of the normally incident wave into a (0, 0)-diffraction wave is diagonal with equal diagonal elements. We can consider the linear polarizations directed along the x and y axes as polarization eigenstates. Any polarization rotation does not appear in this diffraction scenario. Let us note once more that this property is not only the numerical result. It is the rigorous consequence of the reciprocity principle and the symmetry of array. Results of [19, 20] show a polarization rotation by a metal array of finite thickness are not in contradiction with our result related to infinitely thin perfectly conducting arrays.

Variations of intensity s_0 are shown in figures 4 and 5 for linear TE- and TM-polarization of both normally and obliquely incident waves with a dimensionless frequency parameter which is the ratio of the size of the array cell to a wavelength. The rosette array manifests a full resonance reflection at the frequency corresponding approximately to a criterion that half of a wavelength coincides with a stretched length of either crossed strip of the rosette. An incremental number of oscillations appears in the intensity dependences as d/λ increases. The reason is energy redistribution at the frequencies of appearance of new non-evanescent partial waves both in free space and inside the substrate layer, and also resonances inside the substrate due to non-evanescent partial waves propagating at sliding angles. As is evident, intensity variations at oblique incidence of a wave manifest a great complexity due to asymmetry of the partial wave spectrum and therefore a larger number of peculiar frequency values.

For an oblique incidence in the plane xz (the direction of incidence is defined by the azimuth angle $\phi = 0^\circ$ and the incidence angle $\theta = 15^\circ$) and the transmission (reflection)

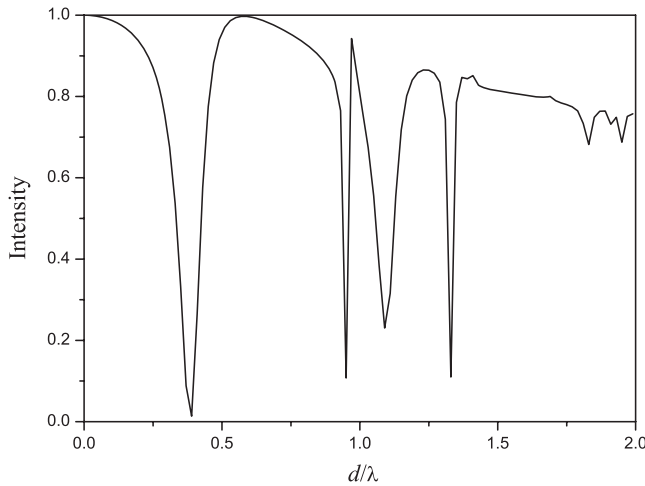


Figure 4. Frequency dependence of $(0, 0)$ -transmitted wave intensity s_0 in the direct diffraction scenario for normal incidence on the array of right-handed rosettes. The intensities of transmitted waves are the same for the TM- and TE-wave incidence.

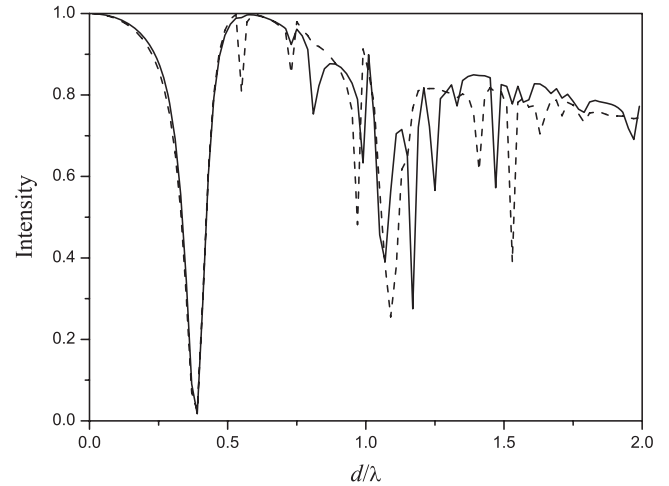


Figure 5. Frequency dependences of $(0, 0)$ -transmitted wave intensity s_0 in the direct diffraction scenario for the oblique incidence in the plane xz ($\phi = 0^\circ$, $\theta = 15^\circ$) on the array of right-handed rosettes. Solid and dashed lines correspond to intensities for the TM- and TE-wave incidence.

into the $(0, 0)$ -diffraction wave in the direct scenario, the matrix T_+ is symmetric (the matrix R_+ is antisymmetric). Two polarization eigenstates of the transmission direct scenario have mutually orthogonal polarization azimuths ($\beta_1 - \beta_2 = 90^\circ$) and the ellipticity angles which are equal in absolute values and signs ($\eta_1 = \eta_2$). The frequency dependences of polarization azimuths and ellipticity angles of the transmission eigenstates are shown in figure 6. An identity of ellipticity signs of two polarization eigenstates differentiates the planar chirality from a bulk volume chirality in diffraction appearances. A three-dimensional chiral medium has two circular polarization eigenstates with opposite handedness of electric field rotation.

Polarization eigenstates of the transmission reversed scenario differ only by the ellipticity signs from the eigenstates of the direct scenario.

Polarization eigenstates azimuths of the reflection direct scenario are not orthogonal but the ellipticity angles differ by signs only ($\eta_1 = -\eta_2$).

Polarization eigenstates of the reflection reversed scenario have the azimuths which are equal by the absolute values and opposite by the signs to the azimuths of the polarization eigenstates of the direct scenario. The ellipticity angles of the reversed scenario polarization eigenstates are the same by absolute values and signs with the corresponding angles of the direct scenario. The reflection direct and reversed scenarios formed by the incident and $(0, 0)$ -reflected waves have mutually orthogonal polarization eigenstates depicted by antipode points on the Poincaré sphere. Thus, the reflection polarization eigenstates are such that the reversed scenario and the direct one are physically indistinguishable. It is also evident from the symmetry of both the array and the reflected rays for any direction of wave incidence.

4.2.2. Normal incidence and the first diffraction order. At first, we will suppose a normal incidence of a wave on the array in the direct scenario. If the wavelength is less than the array period, the diffraction order set appears in the surrounding

space. The polar angle θ_{qp} of the partial wave propagation direction can be found from the expression $\cos \theta_{qp} = \pm \gamma_{qp}/k$ where plus and minus signs correspond to the reflected field and the transmitted one. From the whole set of non-evanescent partial waves, the waves of $(\pm 1, 0)$ - and $(0, \pm 1)$ -diffraction orders propagate in the directions nearest to the array normal. The properties of all wave channels based on these partial waves are identical as a consequence of the fourfold symmetry of the array. Therefore, we will analyze the properties of the wave channel based on the $(1, 0)$ partial wave propagating in the xz plane.

Now let us go to an analysis of polarization transformations as a consequence of diffraction by the chiral array. Frequency dependences of the polarization eigenstates azimuths and ellipticity angles of the direct scenario formed by the normal incident wave and the $(1, 0)$ -diffraction wave are presented in figure 7. Polarization eigenstates azimuths of the direct scenario and the reversed one are different and orthogonal in pairs. We have shown the ellipticity angles for the direct scenario only. The ellipticity angles of the reversed scenario have opposite signs compared with the values in the direct scenario.

The essential difference in polarization eigenstates of the direct wave channel and the reversed one results in the different polarization rotation of an initially linearly polarized wave at direct and reversal propagation. An enantiomorphic array constructed of left-handed rosette-shaped particles has the eigen-polarization azimuths and ellipticity angles differing only by opposite signs from corresponding values related to the array of right-handed particles.

The calculations have revealed that the array of straight crosses (see figure 3(c)) oriented along the main directions of the array ($\psi = 0$) shows the same polarization effect in both the direct and reversed diffraction as in the set of above-mentioned scenarios. Eigenstates of polarization are the same in both directions of diffraction. They are mutually orthogonal in both the direct diffraction scenario and the

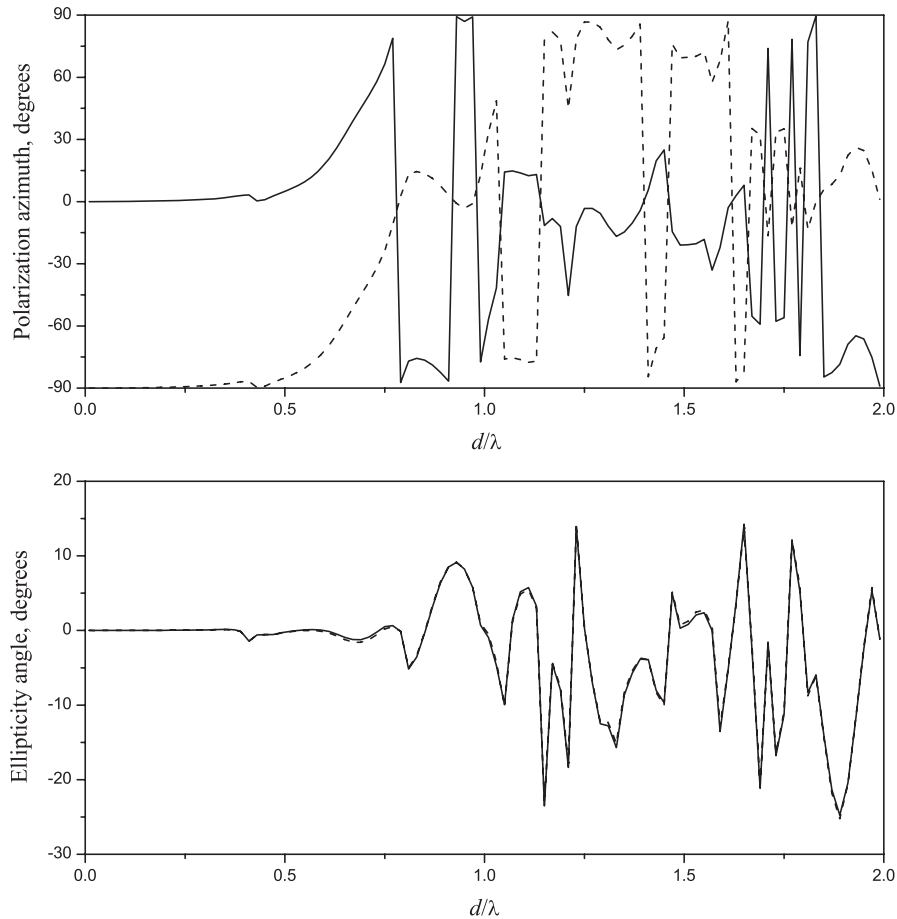


Figure 6. Frequency dependences of azimuths (upper graph) and ellipticity angles (lower graph) of polarization eigenstates of the direct scenario with (0, 0)-diffraction wave for the oblique incidence in the plane xz ($\phi = 0^\circ$, $\theta = 15^\circ$) on the array of right-handed rosettes. Solid and dashed lines correspond to two different eigenstates.

reversed one. However, if the crosses of the two arrays are tilted on angles ψ different from an integer multiple of 45° in opposite (clockwise/anti clockwise) directions, two enantiomorphic forms of the structure are generated, manifesting structural planar chirality. The array of tilted crosses has no plane of symmetry, and is therefore chiral. Polarization transformations are different for waves diffracted on two different enantiomorphic (left–right) forms of the array. Moreover, the polarization eigenstates of the direct diffraction scenario differ from the eigenstates of the reversed scenario for every enantiomorphic form of the array.

The wave diffraction has also been studied in order to find the polarization rotation variation versus the polarization azimuth of the incident wave and geometric parameters of array particles (see [15]). The difference between the polarization azimuths of the eigenstates depends on the rosette bending angle ϕ and reaches a maximum at $\phi = 120^\circ$ for the free-standing array. This difference vanishes at a rosette bending angle equal approximately to 95° . In a diffraction sense, such a rosette array geometry is effectively corresponding to the geometry of the non-chiral array of straight crosses tilted on $\psi = 45^\circ$.

The essential difference in polarization transformations at direct and reverse propagation is also evident when a diffracted

wave is reflected straight back towards the planar chiral structure by a mirror, and is diffracted again. The polarization state of the returning wave after the second diffraction is different from that of the incident wave, even if the incident wave was in an eigenstate in the forward direction [15].

A full transformation of the incident wave into a few diffraction orders or even into a single one is possible with a microstrip rosette array shown in figure 3(e). The frequency dependences of wave normalized intensities presented in figure 8 demonstrate the full transformation of a normally incident wave into four first diffraction orders at the dimensionless frequency which is slightly higher of $d/\lambda = 1.2$. The azimuth and ellipticity angles of polarization eigenstates of the diffraction scenario corresponding to the normally incident wave and the (1, 0)-diffraction one are shown in figure 9. In the reversed scenario, the eigenstate ellipticity angles differ only by opposite signs from corresponding values in the direct scenario.

4.2.3. Oblique incidence and the first diffraction order.

Before studying polarization transformations by diffraction of the obliquely incident wave into the first diffraction order, let us consider a contour diagram presenting regions that correspond to different numbers of non-evanescent partial waves and

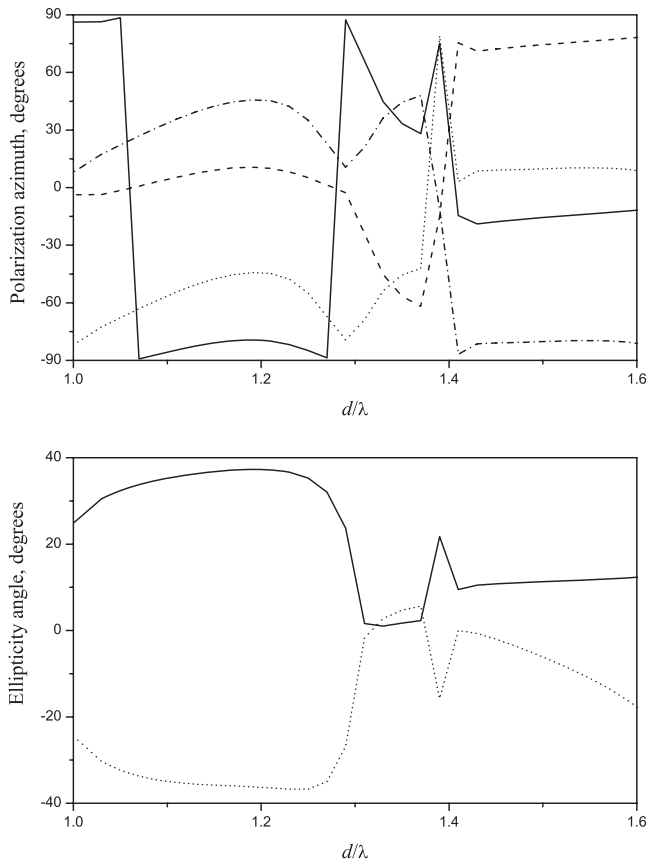


Figure 7. Frequency dependences of the azimuths (upper figure) and the ellipticity angles (lower figure) of polarization eigenstates for the direct and reversed scenarios with (1, 0)-diffraction wave at normal incidence on the array of right-handed rosettes. Solid and dotted lines correspond to the two different polarization eigenstates of the direct scenario while dashed and dotted–dashed lines correspond to the eigenstates of the reversed scenario.

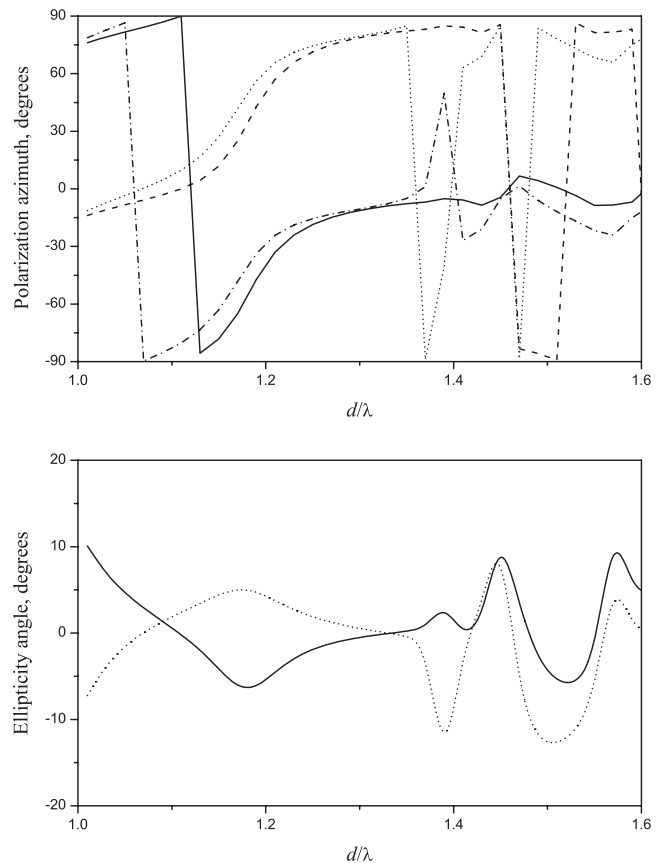


Figure 9. Frequency dependences of azimuths (upper figure) and ellipticity angles (lower figure) of polarization eigenstates of the direct and reversed scenarios with (1, 0)-diffraction wave at normal incidence on the microstrip array of right-handed rosettes. Solid and dotted lines correspond to two polarization eigenstates in the direct scenario. Dashed and dotted–dashed lines correspond to the eigenstates in the reversed scenario.

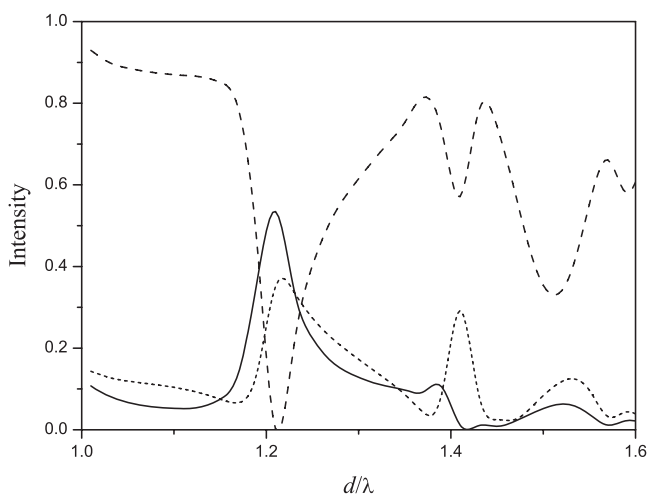


Figure 8. Frequency dependences of normalized intensities of waves reflected by the microstrip array of right-handed rosettes. Solid and dotted lines correspond to an intensity of (1, 0)-diffraction wave for the TM- and TE-wave normal incidence. Dashed line corresponds to an intensity of the main reflected wave for a normal incidence.

depicted on the plane of two variables, being the angle of incidence θ and the normalized frequency d/λ (see figure 10). The contour diagram was drawn under an assumption that the plane xz is the plane of incidence. The leftmost region placed between frame axes and a bold contour line corresponds to the diffraction regime with solely evanescent partial waves. Only the main diffraction order is formed in this region.

In the insulated region bounded by the bold line, the variables correspond to the diffraction regime with the main diffraction order and only one non-evanescent $(-1, 0)$ partial wave. In this region, the incident wave intensity is redistributed between main diffraction orders and $(-1, 0)$ space partial waves of transmitted and reflected fields. The dotted line crossing the bounded region corresponds to a diffraction regime with a propagation of a $(-1, 0)$ partial wave of the reflected field exactly opposite to the direction of an incidence field. It is the autocollimation regime or the Littrow scheme of a diffraction. In the diagram, all lines with the exception of the dotted one correspond to the variables threshold values for transformation of an evanescent partial wave to a non-evanescent one and vice versa. The diffraction leads to the so-called Wood's anomalies at the variable values corresponding to these lines delimiting zones of the diagram.

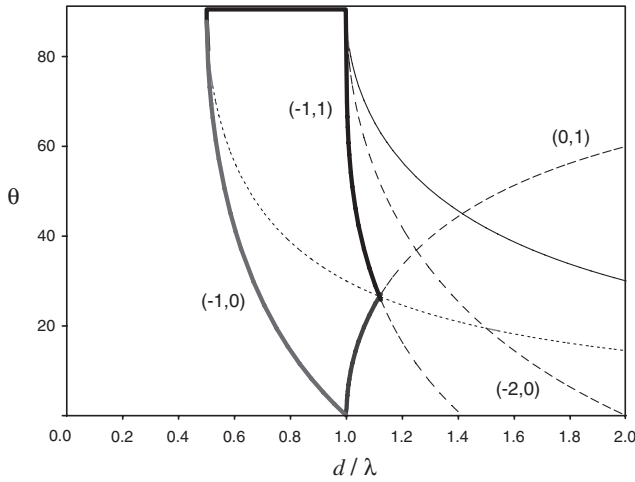


Figure 10. The diagram of regions corresponding to a different number of non-evanescent partial waves on the frame plane of a normalized frequency d/λ and an angle of incidence θ . The region of variable values bounded by a bold line corresponds to a diffraction regime with a main diffraction order and only one non-evanescent partial wave in both a reflection field and a transmission one. The numbers in parentheses denote the lines delimiting the variable regions with the accordingly indexed partial wave being either an evanescent partial wave or a non-evanescent one.

Let us consider a diffraction of a TE-polarized wave on the microstrip array of right-handed rosette-shaped particles. The plane of incidence is xz ($\phi_i = 0^\circ$). The angle of incidence is 25° ($\theta_i = 155^\circ$). In figure 11 we have shown the frequency dependences of values $|a_{00}^{(1)}|^2$ and $|a_{-10}^{(1)}|^2$ for the frequency band with only one non-evanescent $(-1, 0)$ -partial wave. The angle θ_{-10} of $(-1, 0)$ partial wave propagation is varied from 90° up to approximately 29° for this frequency band and the azimuth of its propagation direction is $\phi_{-10} = 180^\circ$. There is a resonance frequency $d/\lambda \simeq 0.93$ corresponding to an essential redistribution of the reflected power between the main specular reflected wave and the partial diffraction wave. The array appears as a non-specular reflecting plane in this frequency. We would like to note that the energy conservation law is satisfied over the whole frequency band including the resonance frequency. Actually, to compare correctly the incoming and outgoing power for any area of the array there is a need to consider the projections of this area on planes normal to the corresponding directions of wave propagation along with the incident and diffraction wave amplitudes. The polarization is close to a linear polarization for both the main specular reflected wave and the partial diffraction wave over the whole considered frequency band. The polarization azimuth of the main reflection wave is $\beta_{00} = -83^\circ$ at the resonance frequency and it is close to 90° far from the resonance. The polarization azimuth of the $(-1, 0)$ partial wave is $\beta_{-10} = 78^\circ$ at the resonance frequency.

5. Conclusion

Vectorial relations of field amplitudes are derived from the reciprocity principle applied to electromagnetic fields at direct

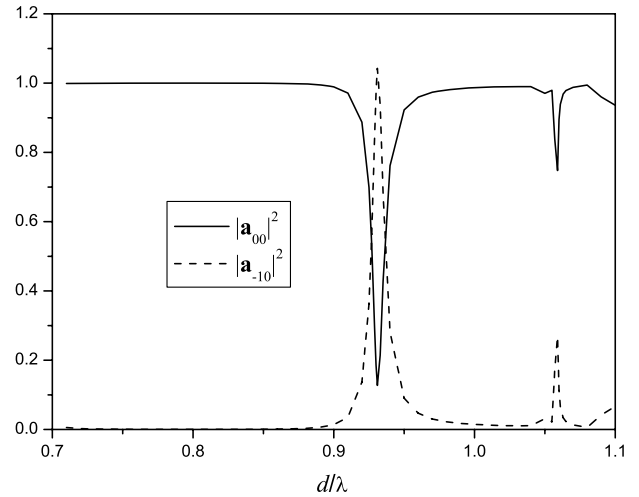


Figure 11. Frequency dependences of normalized intensities of the main specular wave and only one non-evanescent $(-1, 0)$ -diffraction wave reflected by the microstrip array of right-handed rosettes for an oblique incidence of TE-polarized wave in the plane xz ($\phi = 0^\circ$, $\theta = 25^\circ$).

and reversed scenarios of wave diffraction on a doubly-periodic planar array. Biorthogonality of polarization eigenstates of the waves propagating in opposite directions is shown using these reciprocity relations with reference to a wave channel formed by an incident wave and a diffraction order of transmitted or reflected field. The biorthogonality of polarization eigenstates is a general property of wave diffraction by doubly-periodic arrays with any geometry of a periodic cell constructed from linear reciprocal materials.

Some general properties of polarization transformations resulting from an array symmetry are mentioned. It is significant that no polarization rotation is observed in the main diffraction order at transmissive configuration when a wave is normally incident on a fourfold symmetry planar chiral array of infinitely thin perfectly conducting elements placed on a dielectric substrate.

The results of a detailed numerical study of polarization transformations by wave scattering on planar chiral arrays in a resonance frequency range are presented for both transmissive and reflective scenarios. A difference in polarization eigenstates inherent to a planar chiral array and a bulk chiral medium is noticed.

For a planar chiral array, an essential difference in polarization transformations of propagating waves is ascertained for the direct wave channel and for the reversed one. If polarization eigenstates of any diffraction scenario are not mutually orthogonal for the wave channel, a difference in polarization transformations follows from the property of biorthogonality of polarization eigenstates for direct and reversed ray ways. For instance, polarization eigenstates of an asymmetry wave channel based on the incident wave and the first diffraction order are different in the direct and reversed scenarios of diffraction on a planar chiral array. Therefore, a difference in polarization transformations of propagating waves is observed in the direct and reversed wave ways.

Numerical data are also presented to demonstrate the polarization transformations by a reflecting planar chiral array placed on a metal background. Near to full non-specular resonance reflection accompanied by polarization transform action is demonstrated.

Acknowledgments

The authors would like to acknowledge the financial support of the EPSRC (UK), National Academy of Sciences of Ukraine (grant no. 1-02-a) and Metamorphose NoE.

References

- [1] Vardaxoglou J C 1997 *Frequency Selective Surfaces: Analysis and Design* (Taunton: Research Studies Press)
- [2] Munk B A 2000 *Frequency Selective Surfaces: Theory and Design* (New York: Wiley)
- [3] Tretyakov S A, Mariotte F, Simovski C R, Kharina T G and Heliot J-P 1996 Analytical antenna model for chiral scatterers: comparison with numerical and experimental data *IEEE Trans. Antennas Propag.* **44** 1006–14
- [4] Saadoun M M I and Engheta N 1992 A reciprocal phase shifter using novel pseudo-chiral or Ω -medium *Microw. Opt. Technol. Lett.* **5** 184–88
- [5] Mariotte F, Tretyakov S A and Sauviac B 1996 Modeling effective properties of chiral composites *IEEE Antennas Propag. Mag.* **38** 22–32
- [6] Prosvirnin S L and Zouhdi S 2001 Multi-layered arrays of conducting strips: switchable photonic band gap structures *Int. J. Electron. Commun. (AEÜ)* **55** 260–5
- [7] Ziolkowski R W 2003 Design, fabrication, and testing of double negative metamaterials *IEEE Trans. Antennas Propag.* **51** 1516–29
- [8] Cwik T A and Mittra R 1987 Scattering from a periodic array of free-standing arbitrarily shaped perfectly conducting or resistive patches *IEEE Trans. Antennas Propag.* **35** 1226–34
- [9] Cwik T A and Mittra R 1987 The cascade connection of planar periodic surfaces and lossy dielectric layers to form an arbitrary periodic screen *IEEE Trans. Antennas Propag.* **35** 1397–405
- [10] Arnaut L R 1997 Chirality in multi-dimensional space with application to electromagnetic characterisation of multi-dimensional chiral and semi-chiral media *J. Electromagn. Waves Appl.* **11** 1459–82
- [11] Hecht L and Barron L D 1994 Rayleigh and Raman optical activity from chiral surfaces *Chem. Phys. Lett.* **225** 525–30
- [12] Papakostas A, Potts A, Bagnall D M, Prosvirnin S L, Coles H J and Zheludev N I 2003 Optical manifestations of planar chirality *Phys. Rev. Lett.* **90** 107404
- [13] Collin R E 2001 *Foundation for Microwave Engineering* 2nd edn (New York: Wiley)
- [14] Pottin R J 2004 Reciprocity in optics *Rep. Prog. Phys.* **67** 717–54
- [15] Prosvirnin S L and Zheludev N I 2005 Polarization effects in the diffraction of light by a planar chiral structure *Phys. Rev. E* **71** 037603
- [16] Collett E 1993 *Polarized Light: Fundamentals and Applications* (New York: Dekker)
- [17] Gantmacher F R 1998 *The Theory of Matrix* vol 1–2 (Providence, RI: American Mathematical Society)
- [18] Prosvirnin S and Tyrnov D 2004 Polarization transformation by the periodic arrays of complex shaped elements *10th Int. Conf. on Mathematical Methods in Electromagnetic Theory, Conf. Proc. (Dnepropetrovsk, Sept.)* pp 192–4
- [19] Kuwata-Gonokami M, Saito N, Ino Y, Kauranen M, Jefimovs K, Vallius T, Turunen J and Svirko Y 2005 Giant optical activity in quasi-two-dimensional planar nanostructures *Phys. Rev. Lett.* **95** 227401–4
- [20] Konishi K, Sugimoto T, Bai B, Svirko Y and Kuwata-Gonokami M 2007 Effect of surface plasmon resonance on the optical activity of chiral metal nanogratings *Opt. Express* **15** 9575–83
- [21] Prosvirnin S L 1999 Transformation of polarization when waves are reflected by a microstrip array made of complex-shaped elements *J. Commun. Technol. Electron.* **44** 635–40